We are IntechOpen, the world's leading publisher of Open Access books Built by scientists, for scientists

4,800
Open access books available

122,000
International authors and editors

135M
Downloads

Our authors are among the

154
Countries delivered to

TOP 1%
most cited scientists

12.2%
Contributors from top 500 universities

CLARIVATE ANALYTICS BOOK CITATION INDEX INDEXED

WEB OF SCIENCE™

Selection of our books indexed in the Book Citation Index in Web of Science™ Core Collection (BKCI)

Interested in publishing with us?
Contact book.department@intechopen.com

Numbers displayed above are based on latest data collected.
For more information visit www.intechopen.com

Chapter 12

Ionizing Radiation Used in Drug Sterilization, Characterization of Radical Intermediates by Electron Spin Resonance (ESR) Analyses

Şeyda Çolak

Additional information is available at the end of the chapter

http://dx.doi.org/10.5772/61052

Abstract

In this study, the feasibility of radiation sterilization of drugs/drug raw materials is investigated by using Electron Spin Resonance (ESR) spectroscopy. Experimental data and their theoretical correspondings are presented for Sulfanilamide (SA), Sulfafurazole (SFZ), Sulfatiazole (STZ), Sulfacetamide Sodium (SS), Sulfamethazine (SMH), Butylated Hydroxyanisole (BHA), and Albendazole (ALB). Unirradiated samples exhibited no ESR signal whereas the irradiated samples showed ESR spectra consisting of different number of resonance lines indicating that radiolytic intermediates were produced upon irradiation. Increase in the absorbed dose did not create any pattern change in the ESR spectra of these samples. The results of ESR microwave power studies indicated that saturation is observed to be faster for the studies held below room temperatures. Low radiation yield (G=0.1-0.5) calculated by ESR data for the gamma-irradiated samples showed that these materials can not be used as sensitive dosimetric materials. No significant differences were observed between FT-IR spectra of the unirradiated and irradiated samples and this result is considered to be in agreement with the relatively small G value derived from ESR studies. The decay rates of the ESR peak heights of the samples irradiated at different doses and stored at normal and stability conditions were found to be independent of the irradiation doses. The contributing radical species were determined to decay with different decay characteristics and the decay rates but decaying faster at stability conditions. The discrimination of the samples irradiated at even a low absorbed dose from unirradiated samples was possible for a long storage time after irradiation. Cooling the sample temperature down to room temperature did not create any pattern change in the ESR

spectra of irradiated samples except slight reversible increases in the peak heights and at high temperatures irreversible decreases in the peaks heights were observed. Annealing studies indicated that the decay rates of the radical species at high temperatures were higher than the decay rates at low temperatures and the decay activation energies for the radical species were calculated by using Arrhenius plots. Spectrum simulation calculations were also performed and it was concluded that, the molecular ionic fragments and ionic radicals were the main responsible units from the resonance lines of ESR spectra of the gamma-irradiated sulfanomides such as SA, SFZ, STZ, SS, and SMH. Besides these two radical species, some other radical types were also likely produced after irradiation in STZ, SS, and SMH. Besides these two radical species, some other radical types were also likely produced after irradiation in STZ, SS and SMH. As for BHA and ALB, again two other type radical species were believed to produce upon irradiation. Basing on the derived experimental and theoretical data it was concluded that SA, SFZ, STZ, SS, SMH, BHA, and ALB could be safely sterilized by gamma radiation up to permitted drug sterilization radiation doses without causing high amount of molecular damages upon irradiation, and ESR spectroscopy could be used as a potential technique in monitoring the radiosterilization of the drugs, drug raw materials, and drug delivery systems containg present samples as active ingredient.

Keywords: ESR, Radiation Sterilization, Sulfanilamide, Sulfafurazole, Sulfatiazole, Sulfacetamide Sodium, Sulfamethazine, Butylated Hydroxyanisole, Albendazole

1. Introduction

Sterilization is an effective process to eliminate microorganisms such as fungi, bacteria, viruses, spore, etc. from materials. Types of sterilization methods are mainly: "*pressured vapor sterilization*", "*dry heat sterilization"*, "*ethylene oxide (EtO) sterilization"*, *"aseptic sterilization*," and "**radiation sterilization**" [1]. **Radiation sterilization** is based on the exposure of the materials to high-energy ionizing radiation such as *gamma radiation, accelerated beam of electrons*, or *X-ray radiation*.

Sterilization by gamma radiation has been accepted to be a good alternative and an attractive sterilization method for medicinal products and for pharmaceuticals such as drugs/drug raw materials [2-6]. Sterilization by radiation can overcome some specific difficulties that can occur in the other types of sterilization methods. So radiation sterilization method has a general usage on gaseous, liquid, solid materials, homogeneous, and heterogeneous systems [1, 3, 7-9]. Radiation sterilization is also recognized by all major pharmacopeias for pharmaceutical raw materials and their dosage forms are particularly recommended for thermolabile or chemically reactive samples that cannot be sterilized thermally or chemically. With its high penetration range, sterilization by gamma radiation offers some very important advantages such as the possibility of sterilization of drugs

http://dx.doi.org/10.5772/61052

in their final packages (terminal sterilization), low-cost-effectivity, small temperature rise, low chemical reactivity, and ease of validity as the essential validation process is only based on time variable [3, 5, 7-18]. Besides, radiation sterilization is accepted to be a clean, non-residue-producing technology that is safe for the worker and the community. Irradiated drug/drug raw materials are also completely safe to use immediately after sterilization process [2, 3, 10, 14, 18]. Because of these advantages, sterilization by ionizing radiation, especially gamma radiation, has been successfully applied in many countries [13, 21, 22].

EN 552 and ISO 11137 publications recognize standard for implementing radiation technology on sterilization [19, 20]. For the gamma sterilization method, the reference absorbed dose for terminal sterilization is accepted to be **25 kGy**, where the procedures and precautions employed should yield an SAL of at least $\mathbf{10^{-6}}$.

Nevertheless, besides its advantages, radiosterilization also has some drawbacks. Radiation cannot only eliminates microorganisms included in pharmaceuticals but also can cause a molecular decrease in the amount of active drug by destroying it and, therefore, creating reactive molecular fragments which may result in a toxicological hazard [2, 5, 18, 21-24]. Although the radiolytic products induced upon irradiation are generally in very small quantities [14], the characterization of the radio-induced radicals is very important and necessary, both to determine the feasibility of the radiation treatment and to control it. Therefore, to prove the safety of radiosterilization, the determination of physical and chemical features of the radiolytic products and mechanism of radiolysis should be determined [5, 6, 23, 24]. Thus, it is desirable to establish an effective experimental method to discriminate between irradiated and unirradiated drugs as the regulations of irradiated drugs vary from country to country. Besides, radiation effects on drug molecules cannot be generalized; thus, response to ionizing radiation of each molecule has to be individually studied.

Electron Spin Resonance Spectroscopy (ESR), also called **Electron Paramagnetic Resonance (EPR)**, is a spectroscopy technique used particulary for the determination of the types of radiolytical species in paramagnetic samples that contain unpaired electrons, such as organic and inorganic free radicals or inorganic complexes possessing a transition metal ions. Its high sensitivity, precision, ease and its non-destructive readout are the other important advantages of ESR spectroscopy [24-32]. Thus, this nondestructive analytical technique is used for a variety of applications in biology, medicine, and in material science. Moreover, **ESR** is also a very sensitive method for detection of radical intermediates induced in irradiated drug/drug raw materials (radiation sterilized drug/drug raw materials), which appears to be very well suited for their magnetic characterization. ESR yields, both, qualitative information (i.e., whether or not a sample has been irradiated) and quantitative results (i.e., the dose it received), so by this method it is possible to detect and to distinguish irradiated drugs from unirradiated ones.

ESR is a technique that is based on the absorption of electromagnetic radiation in the microwave frequency region by a paramagnetic sample when it is placed in an external magnetic field [32]. ESR resonance can occur basing on the equation (1) where h is the Planck's constant, υ is microwave frequency, g-value is a constant that is dependent on the nature of the radical type ($g = 2.0023$ for a free electron), β is Bohr magneton and H is the applied magnetic field.

$$h\upsilon = g\beta H \quad (1)$$

The results of the ESR studies performed in our laboratory relevant to the structural and thermal properties of the radicals produced in gamma-irradiated **seven** different drugs/drug raw materials will be summarized in the present chapter. The aims of the performed studies were: to investigate the radiation sensitivity of solid drugs/drug raw materials in the dose range of 5-50 kGy through detailed microwave saturation, kinetic and spectroscopic ESR studies and to explore the potential use of ESR technique in monitoring the radiosterilization of the investigated drugs/drug raw materials. Experimental results are presented under two different subsections. The sulfanilamides, which include **Sulfanilamide (SA), Sulfafurazole (SFZ), Sulfatiazole (STZ), Sulfacetamide Sodium (SS), Sulfamethazine (SMH)** and two other drugs/drug raw materials, **Butylated Hydroxyanisole (BHA)** and **Albendazole (ALB)** [16, 33-39].

2. Materials and methods

Samples

The investigated drugs/drug raw materials (Sulfanilamide, Sulfafurazole, Sulfatiazole, Sulfacetamide Sodium, Sulfamethazine, Butylated Hydroxyanisole, Albendazole) were provided from local drug providers and stored at room temperature in a well-closed container protected from light. No further purification was performed and they were used as they were received. Stabilization studies for the samples stored in stability conditions (75% relative humidity; 40°C) were also investigated for some group of drugs.

Irradiation Process

All irradiations were performed at room temperature (293 K) in dark using a ^{60}Co gamma cell supplying a dose rate of ~2.5 kGy/hr as an ionizing radiation source at the Sarayköy Establishment of Turkish Atomic Energy Agency in Ankara, Turkey. The dose rate at the sample sites was measured by a Fricke dosimeter and ESR investigations were performed on samples irradiated at different doses (5 kGy-50 kGy).

ESR Measurements

ESR measurements were carried out using both **Varian 9''-EL X-band** and **Bruker EMX 113 X-Band** ESR spectrometers operating at about 9.5 GHz and equipped with a TE_{104} rectangular double cavity containing a DPPH standard sample (g=2.0036) in the rear resonator which remained untouched throughout the experiments. **The ESR experimental conditions were as follows**; *central field: 350 mT, sweep width: 10 mT; microwave frequency: about 9.85 GHz; microwave power: 0.5-100 mW; modulation frequency: 100 kHz; modulation amplitude: 0.1mT; receiver gain: 5x10^3, sweep time: 83.89 s; time constant: 327.68 ms; conversion time: 81.92 ms; temperature: 100-400 K.* Sample temperature inside the microwave cavity was monitored with a digital temperature control system (Bruker ER 4111-VT). The latter provided the opportunity of measuring the

http://dx.doi.org/10.5772/61052

temperature with an accuracy of ±0.5 K at the site of the sample. A cooling, heating and subsequent cooling cycle was adopted to monitor evolutions of the free radical signals. The temperature of the samples was first decreased to ~100 K starting from room temperature with an increment of ~20 K, then increased to 400 K, and, finally, was decreased again to room temperature. Variations in the line shape and in the signal intensities with microwave power were also studied in the range 0.005-100 mW for samples irradiated at room temperature and at low temperatures. Signal intensities were calculated from first derivative spectra and compared with that obtained for a standard DPPH sample under the same spectrometer operating conditions. Kinetic studies of the contributing free radicals were also performed at different temperatures. To achieve this goal, the samples were heated to predetermined temperatures (320 K-410 K) and kept at these temperatures for predetermined times (3-200 min); then they were cooled to room temperature and their ESR spectra were recorded. The results were the average of five replicates for each radiation dose. Signal intensity variation data obtained for different annealing temperatures were used to characterize the contributing radiation-induced free radicals.

FT-IR Studies

IR spectra of unirradiated and gamma-irradiated samples were also recorded using Nicolet 520 FT-IR spectrometer and a comparison between the principal IR bands of interested drugs/drug raw materials was performed to monitor the radiolytic products silent to ESR spectroscopy.

Simulation

Digitized signal intensity data derived from room temperature ESR spectrum of each sample irradiated at different doses were used as input data for spectrum simulation calculations. The simulation calculations based on models of different tentative radical species anticipating from the results of microwave saturation, variable temperature, decay at normal and stability conditions, dose response, and annealing studies were performed to determine the spectroscopic features of the contributing free radicals.

3. Experimental results and discussion

Experimental results are presented under two different subsections. The sulfanilamides which include **Sulfanilamide (SA), Sulfafurazole (SFZ), Sulfatiazole (STZ), Sulfacetamide Sodium (SS), Sulfamethazine (SMH)** and two other drugs/drug raw materials, **Butylated Hydroxyanisole (BHA)** and **Albendazole (ALB)** [16, 34-39].

Sulfonamides [sulfa drugs: sulfanilamide (SA), sulfafurazole (SFZ), sulfatiazole (STZ), sulfacetamide sodium (SS), sulfamethazine (SMH)] are widely used as antibacterial agents in the treatment of urinary system infections; in meningococcal menengitis prophylaxis; ulcerative colitis; urinary tract infections dysentery; bacterial inflammations of the skin, eye, and the genital area; as well as in veterinary medicine [33]. Sulfonamides were the first substances used to cure and prevent bacterial infections in humans. Investigations on radio-

sterilization of sulfonamides have been rather devoted to the color change determination, loss of potency, formation of acid and gas in irradiated solid and/or aqueous solution samples [33, 40, 41]. As the sulphonamides are known to undergo decomposition during thermal sterilization, radiation sterilization is a preferrable sterilization technique for the sterilization process of sulfanomide drugs/drug raw materials [18]. **Butylated Hydroxyanisole** (BHA) is an aromatic organic compound with the chemical name 2- and 3-tert-butyl-4-methoxy phenol. BHA is used as a preservative and antioxidant in pharmaceutical preparations and cosmetic formulations containing fats and oils [42], as an antioxidant for some rubber and petroleum products, and is a stabilizer for vitamin A. **Albendazole (ALB)** is an antihelminitic drug. Medicines considered in this group are used to treat ruminants by either roundworms or flatworms. Molecular structures of the investigated drug/drug raw materials are given in Table1.

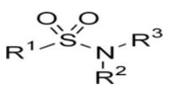 a)Sulfa Drugs	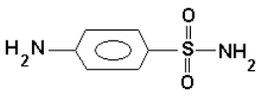 b)SA
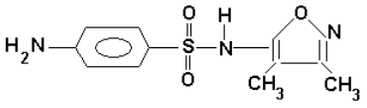 c)SFZ	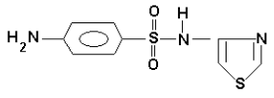 d)STZ
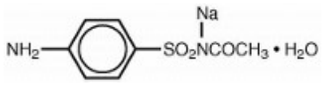 e)SS	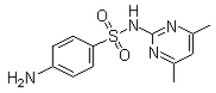 f) SMH
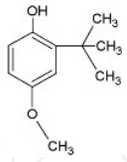 g)BHA	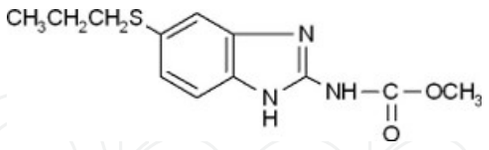 h)ALB

Table 1. Molecular structures of investigated drug/drug raw materials: a) Sulfa drugs, b)SA, c) SFZ, d) STZ, e) SS, f) SMH, g) BHA, h) ALB. (Reproduced from [34], [36], [38], [37], [39] with permissions from Elsevier and Taylor & Francis).

3.1. General features of the ESR spectra

Although unirradiated samples exhibited no ESR signal, irradiated samples showed ESR spectrum consisting of different number of resonance lines depending on the sample investigated [16, 34-39]. The presence of ESR signals in irradiated but not in unirradiated samples is the indication that radiolytic intermediates were produced because of the irradiation mechanism. Increase in absorbed dose did not create any pattern change in the room temperature

http://dx.doi.org/10.5772/61052

spectra of the samples. Thus, it was concluded that irradiation dose was not an important parameter in the formation of the shape of the ESR spectra of the investigated samples in the adopted radiation dose range. The ESR spectra of the investigated samples are given in Figure 1 with their assigned peak numbers for different gamma-irradiation doses.

Irradiated **sulfanilamide (SA)** samples showed a resolved ESR spectrum with g values of 2.0089, 2.0060, 2.0038 (Figure 1-a). **Sulfafurazole (SFZ)** samples irradiated both at *77 K* and *room temperature* showed a very simple ESR spectrum consisting of three resonance peaks appearing at g values of 2.0081, 2.0067, and, 2.0034, respectively (Figure 1-b). **Sulfatiazole (STZ)** irradiated at room temperature showed a complex ESR spectrum consisting of ten resonance peaks (Figure 1-c). The most intense resonance line appearing in the middle of the spectrum was found to have a g value of 2.0045 and a peak-to-peak width of 5.2 G. **Sulfacetamide-sodium (SS)** irradiated showed also a complex ESR spectrum consisting of seven characteristic resonance peaks (Figure 1-d). The resonance peak appearing in the middle of the spectrum was found to have g value of 2.0045 and peak-to-peak width ΔH_{pp}=5.5 G. Irradiated **Sulfamethazine (SMH)** was observed to exhibit an ESR spectrum consisting of one antisymmetric intense central resonance line and three very weak resonance lines at each side of the central line (Figure 1-e). The g values corresponding to the two peaks of the intense resonance line appearing in the middle of the spectrum and its peak-to-peak width were calculated to be 2.0060 and 2.0028, ΔH_{pp}=0.56 mT, respectively. Irradiated **Butylated Hydroxyanisole (BHA)** samples were observed to present an ESR spectrum consisting of three main resonance peaks (Figure 1-f) with g values of 2.0066, 2.0035, and 2.0007, well-developed at high doses with a hardly observed shoulder at low magnetic fields (g=2.0090). Irradiated **Albendazole (ALB)** samples were observed to present a characteristic ESR spectra consisting of three resonance peaks with g values of 2.0041, 2.0105, and 2.0165 (Figure 1-g).

3.2. Microwave power studies

Variations of the signal heights, which were measured with respect to base line and normalized to the receiver gain, masses of the samples, and the intensities of the standart, of these resonance peaks with applied microwave power in the range of 0.5-80 mW, were examined for all the investigated samples. The results of microwave power studies indicated that heights of the assigned peaks increase rather linearly at low microwave powers and saturate homogeneously or inhomogeneously broadened resonance lines at room temperature. Saturation is observed to be faster for the microwave saturation studies which were held below room temperatures. Theoretical functions best fitting to microwave saturation data were calculated assuming *exponentially growing curves* of different characteristics associated with different radical species involved in the formation of experimental ESR spectra of the samples. From the results of these calculations it was concluded that at least *two radical species* of different saturation characteristics were involved for the irradiated samples [16, 34-39].

3.3. Dose-response curves and dosimetric features of the samples

Gamma radiation produces damages in the molecular structures of the irradiated samples where the amount of damage will depend on the absorbed dose level of the sample. From the

experimental results it was concluded that the discrimination of the irradiated samples at a dose as low as 0.5 kGy, from unirradiated samples was possible even long after irradiation due to the relatively high stabilities of the produced radical species, even if gamma radiation yield of the samples is low. A higher concentration of radicals, generated at the same absorbed dose of radiation, indicates a higher sensitivity of the substance toward the type of radiation used. For the samples, variations of the heigths of the resonance peaks assigned as numbers with absorbed gamma radiation doses were generally found to follow a *linear function* such as I=c+bD or a *growth function* such as $I = I_o (1 - e^{-aD})$ in the dose range of 0-50 kGy (Figure 2). In the given equations, "D" stands for the absorbed dose in kGy, "c" is a constant and "a" is the radiation dose growth parameter constant. The calculated different growth rate parameters indicated that more than one radical species contribute to the formation of each resonance peaks. Functions and parameters best fitting to experimental dose-response curves are calculated and given as solid lines in Figure 2.

In the dosimetric studies, G value (*the number of radical species produced by the absorbed radiation per 100 eV*) was also determined for gamma-irradiated solid sulfonomides. This value is calculated to be fairly small (G=0.5 for SA, G=0.45 for SMH, etc.) compared with those reported for sulfonamide aqueous solutions (3.5-5.1) but stay in the range of the G values reported for solid sulfonamides (0.15-0.6) [40, 41]. The big difference in the G values is believed to originate from hydrated electrons (e_{aq}) and hydroxyl radicals (OH) produced in large amount as radiolytical intermediates in irradiated aqueous solutions of sulfonamides. Low radiation yield of gamma-irradiated solid sulfonomides shows that these types of drugs and drug raw material could be suitable candidates for radiosterilization.

3.4. Long-term stability of the radiation-induced radicals

Room temperature stabilities of the radicals induced in the irradiated drugs/drug raw materials upon irradiation are as important as the radiosensitivity of these materials. ESR spectra of the samples which were open to air, were recorded in regular time intervals over a long period of time (approximately, 3 months) without changing the position of the sample in the microwave cavity throughout the experiment on normal conditions (*room temperature and normal pressure in the air*). Besides storing at normal conditions, for only the samples of SFZ, STZ, and SS, the decay rates of the samples irradiated at different doses were also investigated for storing at stability conditions (*40°C and 75% relative humidity*). The signal intensity decay data obtained for the samples irradiated were used to get the decay characteristics of the contributing radicals. The decay constants derived from this study for SA, STZ, SS, and BHA are summarized in Figure 3 and theoretical decay results calculated using these parameters are given together with their experimental counterparts (Table 2).

The decay of the peak heights of the samples irradiated at different doses and stored in well-closed container at normal and stability conditions was found to be independent of the irradiation dose. Contributing radicals were determined to decay much faster at stability conditions. The peak heights or spectrum area were observed to experience fast decreases during the beginning of the storage period; after the first days of storage, the decay rate of the induced radicals in the samples upon irradiation was decreased. Model based on the assump-

http://dx.doi.org/10.5772/61052

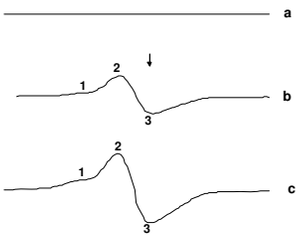

***SA: a)** Unirradiated, **b)** 10 kGy, **c)** 50 kGy*

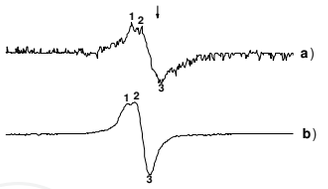

***SFZ: a)** 5 kGy, **b)** 50 kGy*

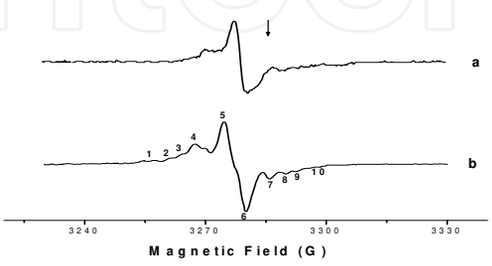

***STZ: a)** 5 kGy, **b)**50 kGy*

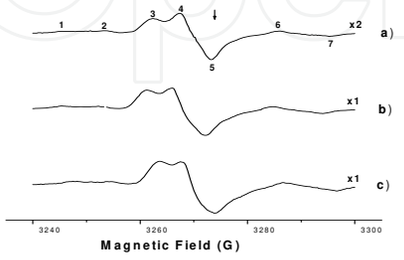

***SS: a)** 1 mW; **b)** 10 mW; **c)** 40 mW.*

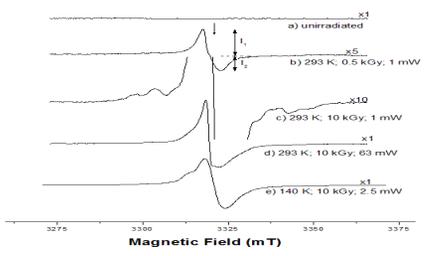

***SMH:** recorded at different temperatures and microwave powers.*

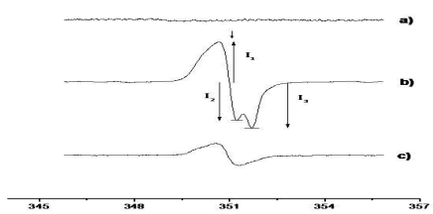

***BHA: a)** unirradiated, **b)** just after and **c)** 17 days after irradiation at 10 kGy.*

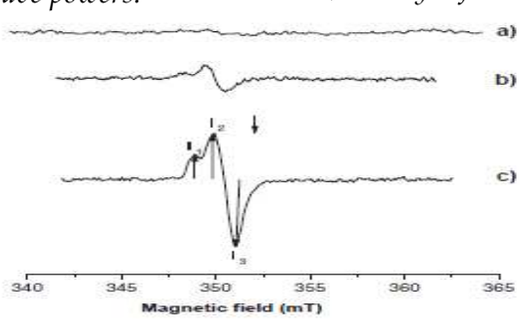

***ALB: a)** unirradiated, **b)** 3 kGy, **c)** 34 kGy*

Figure 1. Room temperature ESR spectra of SA, SFZ, STZ, SS, SMH, BHA, ALB. Arrow indicates the position of DPPH (standart sample) line. (Reproduced from [34], [36], [16], [38], [37], [39] with permissions from Elsevier and Taylor & Francis).

tions that different numbers of radicals for each sample with different decay kinetics were produced and that they undergo *first-order decay kinetics* was tried to describe the experimental decay data. That is, calculated experimental peak heights were fitted to the equation $I(t)=I_{oA}\,e^{-kAt}+I_{oB}\,e^{-kBt}+I_{oC}\,e^{-kCt}+I_{oD}\,e^{-kDt}+\ldots$ comprising different number of first-order decay terms with

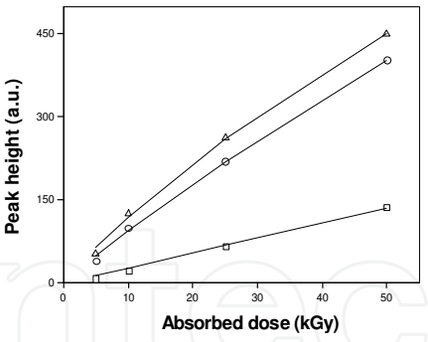

SA: *□ (line1), Δ (line 2), o (line 3)*

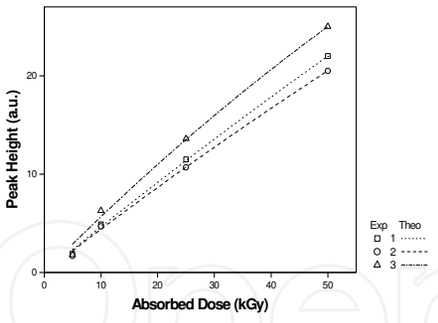

SFZ: *⊠ (peak 1), o (peak2), Δ (peak 3).*

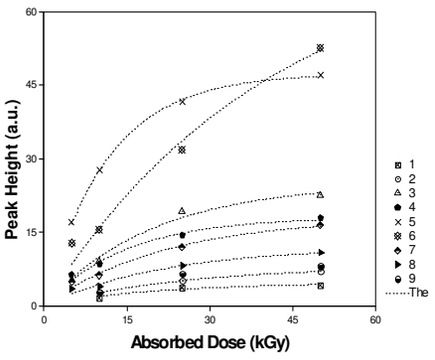

STZ

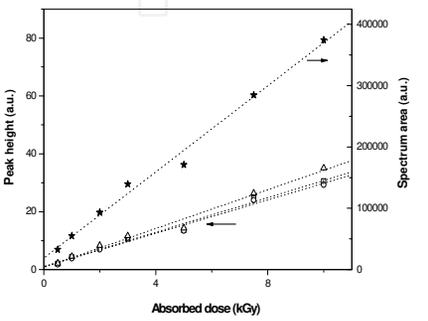

BHA: *I_1 (□); I_2 (o); I_3 (Δ); spectrum area(✶).*

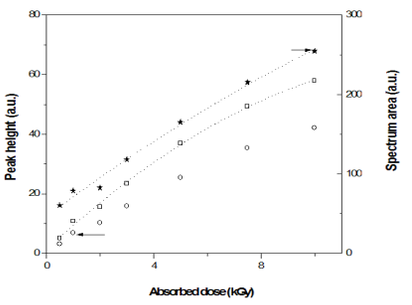

SMH: *I_1 (□); I_2 (o); spectrum area (✶).*

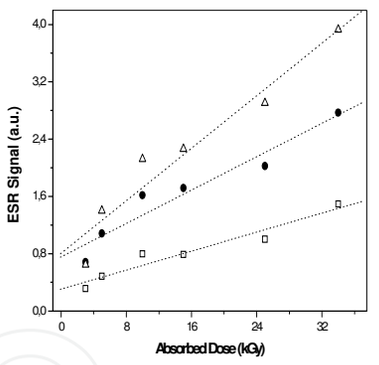

ALB:. *I_1 (□); I_2 (●); I_3 (Δ).*

Figure 2. Dose-response curves for SA, SFZ, STZ, SMH,BHA, ALB. Symbols: experimental; solid line: theoretical curves best fitting to experimental data. (Reproduced from [34], [36], [38], [37], [39] with permissions from Elsevier and Taylor & Francis).

different decay constants and different weights. In the equation, t, I_{os}, and k_s stand for the time elapsed after stopping irradiation, the initial signal intensities, and decay constants, respectively, for the contributing radical species in the samples. As the signal height decay data of different resonance lines were calculated to fit to the different exponential functions with different relative weights and decay constants, this result indicated that more than one radical species were induced upon irradiation in the samples which have different decay characteristics.

http://dx.doi.org/10.5772/61052

For SA samples, a slight increase in the height of line 1 at the beginning of storage period was the common behavior of the samples irradiated at different doses and stored at room temperature. This likely originates from the transformation of the radicals dominating line 2 and 3 to the radical giving rise to line 1 (Figure 3). **For STZ samples**, the decays over a period of 90 days of the peak heights of the samples stored at normal conditions were calculated best fitting to the sum of four exponentially decaying functions of different weights and of different decay constants. **For SS samples**, the data for the samples stored both at normal and stability conditions were found best fitting to the sum of four exponentially decaying functions with different decay constants. Peak heights of irradiated SS decreased ~90 % in the first 20 days after stopping irradiation when stored in stability conditions. For **BHA sample**, the model based on the presence of two different radical species undergoing first-order decay kinetics describes fairly well the experimental room temperature long-term decay data of this sample. For 25 kGy irradiated **SMH samples**, at the end of storage period of 40 days at normal conditions, a decrease of 10% of signal intensity is observed where it is an indication that the induced radical species upon irradiation in SMH are fairly stable at normal storage conditions. For 34 kGy irradiated **ALB sample** which is stored at normal conditions, at the end of 40 days of storage period the signal intensities of the peak height were decreased to 70% and it was ~85% at the end of 200 days. The discrimination of irradiated Albendazole from unirradiated one was possible even 6 months stored at normal conditions. The decay constants calculated for each sample for the related resonance signal is given in Table 2.

3.5. Variable temperature study

The results of variable temperature studies found from the variations of the peak heights with temperature in the range of 290-110 K and 295-400 K are given in Figure 4. The sample was first cooled down starting from room temperature with an decrement of 20 K. Then, the temperature was increased up to high temperatures with the same increment. Spectra were recorded ~5 min after setting the temperature. For the irradiated samples, cooling the sample down to room temperature did not create any pattern change in the spectra except slight reversible increases in the peak heights likely due to classical paramagnetic behavior of the contributing species, as obeying Curie's Law. But irreversible decreases in the intensities at high temperatures were observed for the samples. **For SA sample**, the increase in temperature produced no significant change in the peak heigths of the resonance lines up to 320 K. However, warming the sample above this temperature caused continous decreases in the peak heights of the resonance lines 2 and 3, but it created a slight increase in the height of line 1, up to 375 K, and then a relatively sharp decrease occurred. **For SFZ sample,** the increase of the sample temperature above 320 K caused continuous decreases in the heigths of the resonance peaks up to 360 K, and then a relatively sharp decrease in the heights occurred. **For STZ sample,** relatively sharp decreases especially in the heights of 5^{th} and 6^{th} peaks were observed for the sample temperature above 320 K. Above ~370 K, ESR spectrum of STZ turned into a singlet resonance line, indicating that most of the radical species were decayed completely at high temperatures, except that or those contributing to the central line (g=2.0045). **For SS sample**, warming the sample above room temperature produced no significant changes in the heights of the observed peaks where this result is accepted to be orginating from the high stabilities

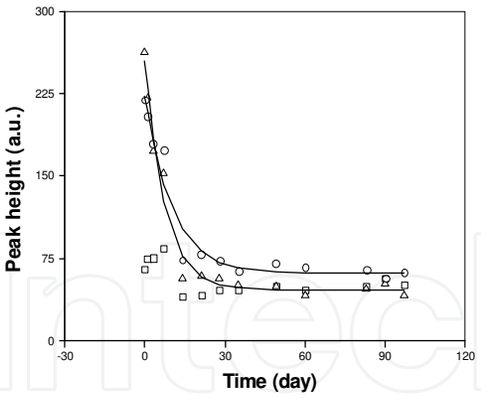

***SA** irradiated at a dose of 25 kGy. Symbol:experimental [□ (1), Δ (2), o (3)].*

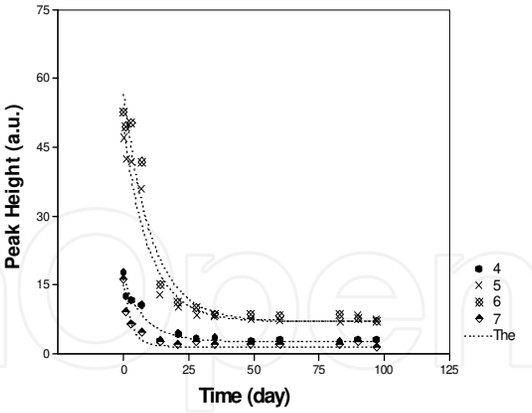

***STZ** irradiated at a dose of 50 kGy.*

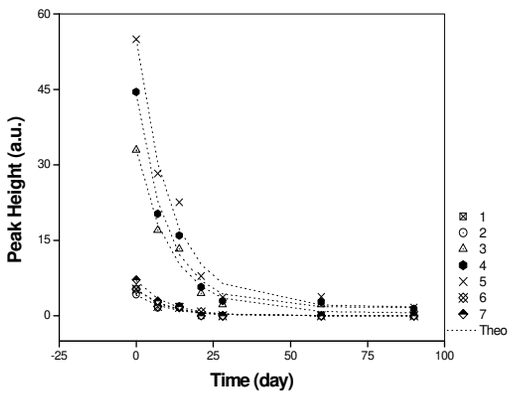

***SS** irradiated at a dose of 50 kGy and stored at stability conditions.*

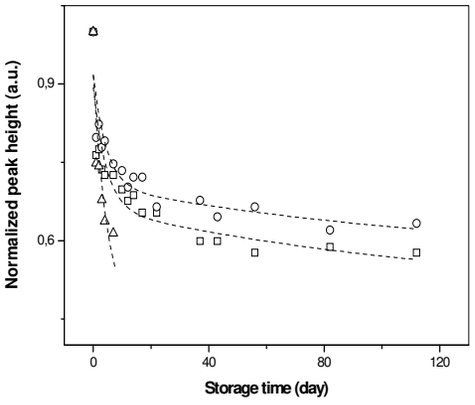

***BHA** irradiated at a dose of 34 kGy. I_1 (□); I_2 (o); I_3 (Δ).*

Figure 3. Variations of ESR signal intensities of SA, STZ, SS, and BHA samples irradiated at different dose levels and stored over a long period of time. symbols: experimental; solid lines: theoretical. (Reproduced from [34], [36], [16], [38] with permissions from Elsevier and Taylor & Francis)

of the radical species induced in SS, probably because of the existing higher cage effect in its lattice. **For SMH sample**, relatively sharp drops were observed above 370 K. The slight increases of the peak heights in the range of 295-350 K were evaluated as originating from the decay of the radical species giving rise to weak satellite lines taking part at both sides of the central intense resonance line. **For BHA sample**, sharp irreversible decreases in the studied heights, related with important radical decays, were observed above 310 K. **For ALB sample**, irreversible decreases in the heights of all peaks, related with important radical decay, were also observed above room temperature.

3.6. Radical decays in annealed samples

Basing on the drastic decreases observed in the peak heights of the samples above room temperature, annealing studies were also performed to determine the kinetic features of the radical species which were responsible from experimental ESR spectra of gamma-irradiated

http://dx.doi.org/10.5772/61052

SA*(stored at normal conditions)*					**STZ***(stored at normal condition)*		
I	**Radical Species**	**Relative weightk (day^{-1})**		**r^2**	**Radical Species**	**Decay constants(r^2) kx10^5 (day)$^{-1}$**	
2	A	48.11 (±19.65)	0.00053 (±0.00002)	0.98	A	1483 (±107)	0.98
	B	201.64 (±20.49)	0.14487 (±0.03659)		B	8400 (±420)	
					C	1178 (±95)	
					D	9800 (±450)	
3	A	70.84 (±6.27)	0.00053 (±0.00002)	0.94			
	B	155.24 (±13.02)	0.14487 (±0.03659)				

SS *(stored at normal and stability conditions)*			**BHA** (*stored at normal conditions)*		
Radical Species	**Decay constants kx10^5 (day^{-1}) Normal Stability Condition Condition**	**r^2**	**Radical Species**	**Relative Weights $I_{1\ 3}$**	**k (day)$^{-1}$**
A	3 9901	0.98	A	0.4219 0.3996	0.008
B	(±1) (±285)	0.99		0.6062	
C	2 7856				
D	(±1) (±200)				
	46 11764				
	(±5) (±325)				
	167 9677				
	(±13) (±210)				
			B	0.5181 0.6004	0.224
				0.3938	
				±0.8484 ±0.8731	
				±0.8193	

Table 2. Decay constants for contributing radicals calculated for SA, STZ, SS, and BHA. (Reproduced from [34], [36], [16], [38] with permissions from Elsevier and Taylor & Francis).

samples and calculating the activation energies relavant to the radical decay processes. Investigation of the contributing radical species by using ESR signal intensities in annealed samples is very important from the kinetic point of view. The fact that radical decay rates depend on the nature of the matrix containing radicals and annealing is a constant process with local diffusion of radicals and molecules in some softening of defects or irregularities [43]. At room temperature, the decay is very slow and many radical-molecule reactions observed in the liquid state are not observed in the solid state. Irreversible decreases in the intensities at high temperatures would be expected to originate from the decay of the radical species.

Thus, irradiated samples were annealed at different temperatures above room temperature; that is, below their melting temperature range for predetermined times. The decay rates of the radicals at high temperature are found to be higher than the decay rates at low temperatures.

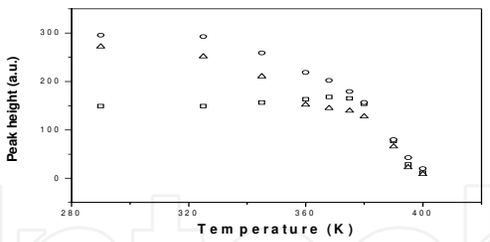

SA: *□ (line 1), Δ (line 2), o (line 3).*

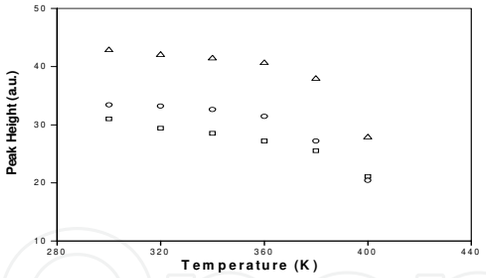

SFZ: *⊠ (line 1), o (line 2), Δ (line 3).*

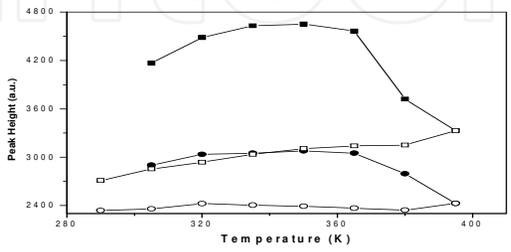

SS: *□ (line 1); o (line 2). Bolds: heating; open: cooling.*

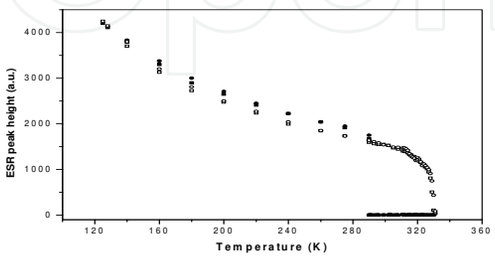

BHA: *□ (line 1); o (line 2). Bolds: cooling; open: heating.*

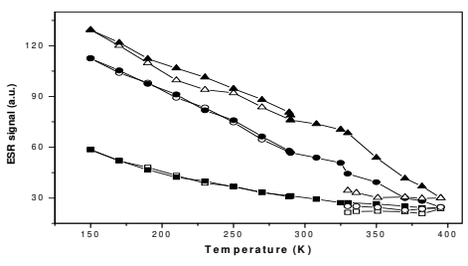

ALB: *□ (line 1); o (line 2); Δ (line 3). Bolds: heating; open: cooling.*

Figure 4. Variation of peak heights of SA, SFZ, SS, BHA, ALB with temperature. (Reproduced from [34], [36], [38], [37] with permissions from Elsevier and Taylor & Francis)

Signal intensity decay results obtained for the samples irradiated at different doses and annealed at different temperatures for different times were used to get the decay curves of the resonance lines (Figure 5). Experimental peak height decay data obtained for the samples annealed at different temperatures were used to calculate the decay constants of the contributing species at the annealing temperatures, assuming that radical species induced upon irradiation follow a *first-order kinetics* as in the equation $I(t)=I_{oA}\, e^{-kAt} + I_{oB}\, e^{-kBt} + I_{oC}\, e^{-kCt} + I_{oD}\, e^{-kDt} + \ldots$ where t, I_{os}, and k_s stand for the storing times at the initial signal intensities, and decay constants, respectively, for the contributing radical species.

For SA sample, the radiation-induced radicals in the sample were observed to be very unstable even at room temperature. The decreasing rate of the intensities of the different peak heights indicated that there are more than one responsible induced radical species in the sample. All peaks suffer drastic intensity decreases above 365 K and the longer the annealing time the higher the intensity decrease. **For SFZ sample,** the signal intensity decay results obtained for

http://dx.doi.org/10.5772/61052

peak 3 of a sample irradiated at a dose 50 kGy and annealed at different temperatures for different times indicated that two radical species with different decay constants were found to fit best the experimental signal intensity decay data. **For STZ sample,** the annealing results relative to the height of peak 5 of a sample irradiated at a dose of 50 kGy are best fitted to a model of four radical species with different decay constants. **For SS sample,** four radical species are found to be responsible for the peak 4 of the SS spectrum, which is irradiated at 50 kGy. **For SMH sample,** the variations of the peak 2 for a sample irradiated at a dose of 10 kGy indicated that a model predicting the presence of three radicals undergoing first-order kinetics were explaining the decay data very well. **For BHA sample**, variations of the peak 2 for a sample irradiated at 10 kGy indicated that side radical species decayed differently at room and at high temperatures. That is, up to the lower limit of melting region (~321 K) the decay is very slow, but in the melting temperature range (321-338 K) the decay rate of the radicals are much faster. **For ALB sample,** the decay rates of I_2+I_3 peak heights of sample irradiated at 34 kGy, which was annealed, indicated that a model of two radical species could be used best in the fitting process of the experimental decay data recorded. An Arrhenius plot was also constructed to determine the activation energies of the contributing radical species for each irradiated sample. The activation energies are calculated from the slopes of the straight lines of ln(k) = f (1/T) of the Arrhenius plot constructed by using decay constants given in Table 3.

STZ				SS			
Ann. Temp. (K)	**Type**	**kx10^5 (min)$^{-1}$**	**r^2**	**Ann.Temp. (K)**	**Type**	**kx10^5 (min^{-1})**	**r^2**
310	A	9 (±1)	0.96	358	A	9 (±1)	0.98
	B	52 (±7)			B	7 (±1)	
	C	10660 (±325)			E	69 (±4)	
	D	2451 (±95)			F	31 (±3)	
348	A	59 (±8)	0.97	393	A	1436 (±115)	0.99
	B	380 (±30)			B	1234 (±80)	
	C	27000 (±430)			E	2755 (±180)	
	D	11000 (±360)			F	1257 (±105)	
365	A	344 (±45)	0.98	413	A	4536 (±185)	0.99
	B	1230 (±75)			B	3547 (±155)	
	C	46000 (±550)			E	7215 (±220)	
	D	17000 (±280)			F	5390 (±205)	
393	A	1575 (±105)	0.99				
	B	5500 (±120)					
	C	68000 (±310)					
	D	35200 (±180)					
413	A	**1675 (±120)**	**0.99**				
	B	**6462 (±110)**					

	C	102000(±220)
	D	56207 (±205)

SMH				ALB			
Ann. Temp. (K)	**Type**	**kx10³ (min⁻¹)**	**r²**	**Ann. Temp. (K)**	**Type**	**kx10³ (min⁻¹)**	**r²**
365	A B H	0.9 3.6 80.0	0.99	370	L M	118.65 3.17	0.98
375	A B H	1.1 7.9 180.3	0.99	380	L M	127.71 6.99	0.99
385	A B H	3.7 67.8 221.2	0.99	390	L M	172.71 7.43	0.97
390	A B H	4.5 118.1 389.2	0.99	400	L M	397.14 12.16	0.95
395	A B H	10.7 212.6 440.1	0.99				

Table 3. Decay constants at different temperatures for the radicals contributing to the ESR spectra of the irradiated STZ, SS, SMH, ALB. (Reproduced from [34], [36], [16], [38] with permissions from Elsevier and Taylor & Francis).

3.7. Radical type

Excited molecules are produced both directly and through radical-cations neutralization reactions [44]. They may decompose to radicals by rupture of chemical bonds. However, all species produced after irradiation are expected to undergo immediate germination termination reactions [43] due to cage effect. Consequently the amounts of the species responsible from the ESR spectra would be different depending on the capacity of these species participating to the germination reaction. Excited molecules and, as a result, radicals are localized along the track in region of high local concentration.

3.7.1. Proposed radical species for sulfanomides: SA, SFZ, STZ, SS, SMH

It is believed that the **molecular ionic fragment** (radical A) and **[O=S=O]* ionic radical** (radical B) are the main responsible units from the resonance lines of ESR spectra of the gamma-irradiated sulfanomides of SA, SFZ, STZ, SS, and SMH. These two radical species were assumed to be produced upon irradiation and giving rise to *isotropic* and *axially symmetric* ESR spectra of the sulfanomide samples. Experimental g values determined in the studies for the

http://dx.doi.org/10.5772/61052

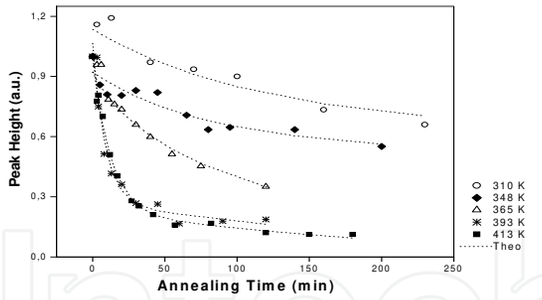

*Peak 5 of 50 kGy irradiated **STZ** and annealed at ○ (310 K), ♦ (348K), Δ (365 K), ж (393 K), ■ (413 K).*

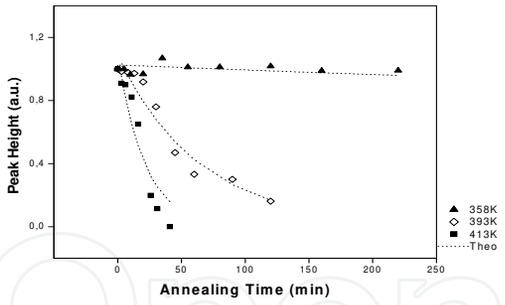

Peak 4 of 50 kGy irradiated SS and annealed at ▲(358K), ◊(393K), ■Δ (413K).

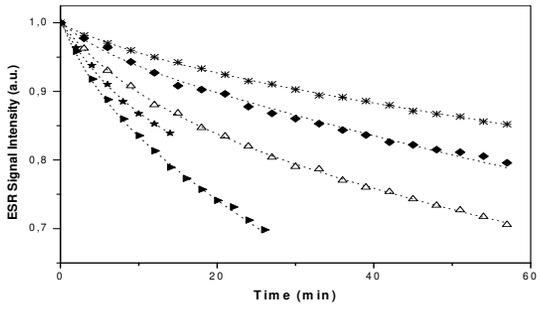

Peak 2 of irradiated smh with annealing 365K (✵); 375 K (◆); 385 K (Δ); 390 K (★); 395 K (►).

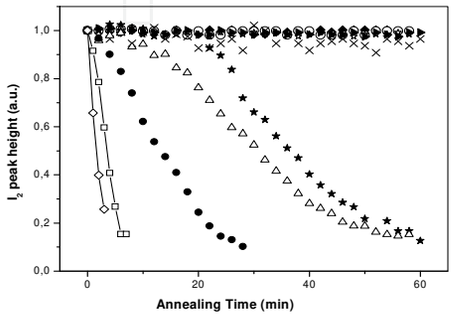

Peak 2 of BHA with annealing 300 K (◆); 308 K (⊙); 312 K (☆); 318 K (►); 320 K (x); 326 K (★); 327 K (Δ); 328 K (●); 329 K (□); 330 K (◊).

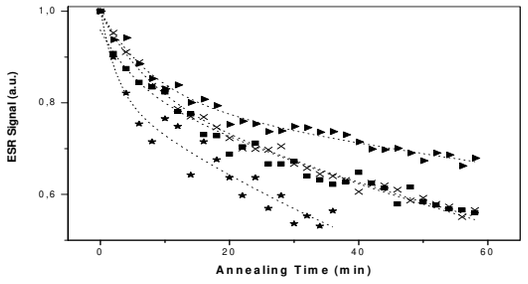

Variations of the peak height of 34 kGy irradiated ALB with annealing 370 K (►); 380 K (x); 390 K (■); 400 K (★).

Figure 5. Decay results for the resonance lines of the irradiated samples at different dose levels and annealed at different temperatures for different times. Symbol: experimental, line: theoretical curves. (Reproduced from [36], [16], [38], [37], [39] with permissions from Elsevier and Taylor & Francis).

resonance peaks of the gamma-irradiated samples fall into the expected g value range where sulfur radicals do not exhibit hyperfine structure. The unpaired electron in **SO_2^- ionic radical** (radical A) occupies the antibonding $2b^*$ orbital formed from p orbitals of the S atom. Radicals A and B produced upon irradiation in powder of investigated sulfanomides are randomly oriented and the motion of radical A is restricted in large extent due to the big group attached to it, so that it give rise to powder ESR spectra with principal g values varying between g_{xx}=2.0022-2.0031, g_{yy}=2.0015-2.0098, and g_{zz}=2.0058-2.0066 [45, 46]. As for SO_2^- ionic radical (radical B), its motional freedom is high due to very weak steric effect experienced by this

radical and it gives rise to a single resonance line of average spectroscopic g factor varying between 2.0037-2.0059 [44-46].

For SA and SFZ samples, only the two radical species (A and B) are assumed to be induced upon irradiation but the spectral parameters of these radical types are different depending on the different lattice specifications of the samples (Table 4). **For STZ sample**, besides these two radical types named A and B, other two types of radical species are also likely produced after hemolytic ruptures of **S-N** (radical C) and **C-S** (radical D) chemical bonds in the irradiated STZ. **For SS sample**, in addition to radical species A and B, (radical E) and (radical F) were found to be involved in the irradiated SS. Radical E is formed after the break of N-Na bond and it has hyperfine splittings as the unpaired electron is localized on nitrogen atom. However, methyl radical is formed after the break of C-C bond and its unpaired electron is expected to be localized on the carbon atom. It has four peaks with 1:3:3:1 relative weight due to the methyl hyrogens. **For SMH sample**, besides the radical species of A and B, a third different radical species (radical H) is also assumed to be responsible from the very weak satellite peaks taking part at both sides of the central intense line which is believed to be produced after hemolytical rupture of **S-N bond** causing the creation of a species having unpaired electron localized rather on nitrogen atom and interacting with an alpha proton. That is, a species of type, which is assigned as **H**.

3.7.2. Proposed Radical Species for BHA and ALB

For BHA samples, species exhibiting single isotropic resonance line is believed to result after removing hydroxyl hydrogen from the molecule. This gives rise to a radical (radical J) with unpaired electron localized on hydroxyl oxygen and not interacting with any hydrogen of the molecule. It is denoted **radical J** in the present work. Second species (radical K) is likely formed by removing one of the neighboring ring hydrogen atoms on ortho or para position conducting to the formation of the radical with unpaired electron localized on one of the ring carbon atoms. Unpaired electron of this species exhibits an axial hyperfine interaction with its nearest neighbor ring hydrogen atom due to planar nature of the ring. Second species is denoted **radical K** in the present work. They are proposed to be produced by removing hydroxal and one of the ring protons from the molecule. Their production is preferential. **For ALB samples, radical L** and **radical M** are believed to be created by dissociations of S-H bonds and one of the C-H bonds at the position five or six on the benzene ring, respectively. Dissociations of S-H bonds create species with unpaired electron localized on sulfur and dissociation of C-H bonds creates species with unpaired electron localized on carbon atom. The neighboring protons to sulfur atoms gives rise to line broadening in species L.

3.8. Spectrum simulation calculations and proposed tentative radical species

Simulation calculations were performed to support the idea put forward with the species responsible from the observed experimental resonance peaks of ESR spectra of gamma-irradiated samples and to determine correct spectroscopic parameters of the contributing species. For the simulation calculations, the room temperature experimental signal intensity data obtained from the ESR spectra of the irradiated sample were used as input to perform simulation calculations. A model of different numbers of radical species depending on the

http://dx.doi.org/10.5772/61052

samples was adopted throughout the calculations. Spectral parameter values determined by this technique for contributing radical species and theoretical ESR spectra calculated using the corresponding experimental counterpart are presented together in Table 4. The agreement between experimental and theoretical spectra is fairly good, which indicates that the modelings based on the expected species of different characteristic features explains well the experimental ESR spectra of gamma-irradiated samples.

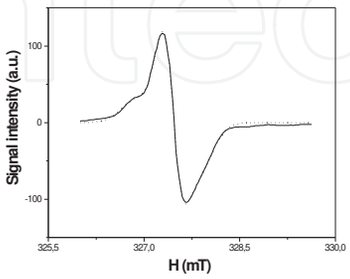

SA

Radical Species	Relative Weight	Line width (G)	g factor
A	7.32	2.43	g_{II}=2.0089 $g_{\perp}$=2.0035
B	226.47	1.59	g_{av}=2.0052

SA *(solid line: experimental; dashed line: theoretical).*

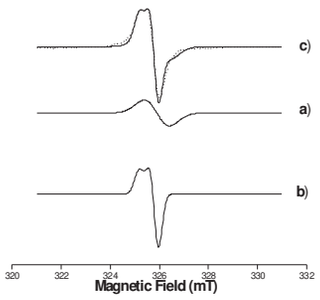

a) *Experimental and calculated ESR spectra for irradiated* ***SFZ****,* ***b)*** *calculated spectra for radical species* ***A*** *and* ***B****, respectively,* ***c)*** *experimental and calculated sum spectra.*

SFZ

Radical Species	g factor	Line Width (G)	Relative Weight
A	2.0042	5.10	0.52
B	2.0090 2.0047	1.78	0.48

Experimental and calculated ESR spectra for irradiated ***STZ.*** *Solid line: theoretical, dashed line: experimental*

STZ

Radical Species	g factor	Line Width (G)	A_N AH (G) (G)	Relative Weight
A	2.0051	1.5	- -	0.06
B	2.0106 2.0030	1.4	- -	0.21
C	2.0059	0.8	13.7 3.6	0.01
D	2.0039	8.0	- 3.2	0.73

SS

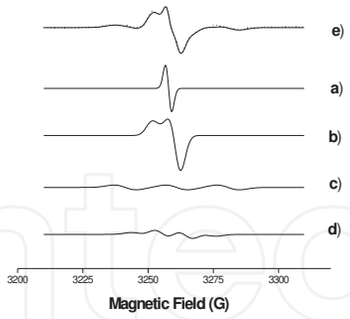

*Experimental and calculated ESR spectra for **SS** irradiated at a dose of 50 kGy. **a), b), c), d):** calculated spectra for radical species A, B, C and D, respectively. **e):** experimental and calculated sum spectra.*

Radical Species	g factor	Line Width (G)	Hyperfine Splitting A (G)
A	2.0052	1.21	-
B	2.0092 2.0031	2.15	-
E	2.0033	4.25	19.7
F	2.0040	3.50	8.6

SMH

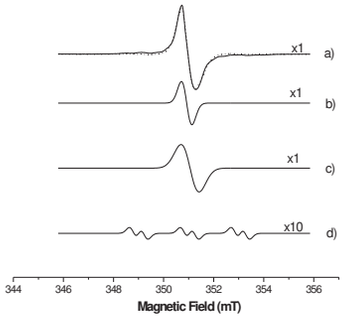

*Experimental (solid line) and theoretical (dashed line) ESR spectra of irradiated **SMH**. **a)** sum spectra, **b)** species A; **c)** species B; **d)** species H*

Radical Species	g factor	Line Width (G)	Hyperfine Splitting A_N(mT) A_H(mT)	Relative Weight
A	2.0072	0.21	- -	0.47
B	2.0059 2.0075	0.35	- -	0.51
H	2.0066	0.16	2.03 0.21	0.02

BHA

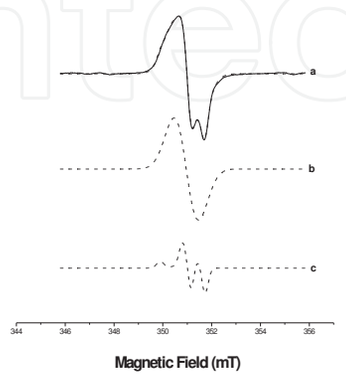

Radical Species	g factor	Line Width (G)	Hyperfine Splitting A_N(mT) A_H(mT)	Relative Weight
J	2.0057	0.50	- -	0.834
K	2.0047 2.0067	0.14	0.1584 0.9009	0.166

http://dx.doi.org/10.5772/61052

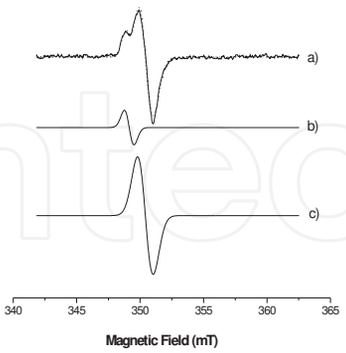

*Experimental (solid line) and theoretical (dashed line) ESR spectra of irradiated **BHA.a)** sum spectra; **b)** species J; **c)** species K.*

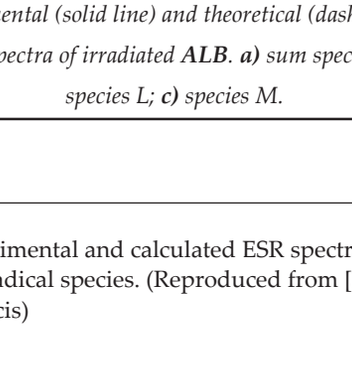

*Experimental (solid line) and theoretical (dashed line) ESR spectra of irradiated **ALB**. **a)** sum spectra; **b)** species L; **c)** species M.*

Radical Species	g factor	Line Width (G)	Relative Weight
L	2.0161	3.8	0.10
M	2.0088	6.16	0.90

Table 4. Experimental and calculated ESR spectra for irradiated samples and calculated spectral parameters for contributing radical species. (Reproduced from [34], [36], [16], [38], [37], [39] with permissions from Elsevier and Taylor & Francis)

For SA sample, a model of **two radical species** was adopted throughout the calculations. Although the line width of radical B is small, it dominates ESR spectrum and radical A contributes mainly to the line centered at g=2.0089. **For SFZ sample,** the line width of species B is small compared with ionic radical A, but both species equally dominate ESR spectrum. **For STZ samples,** simulation calculations were performed assuming the presence of four radical species, exhibiting isotropic (species A, C, and D) and axially symmetric (species B) g tensors. Linewidth and relative weight of the radical D are found to be fairly large compared with other radical species due to unresolved hyperfine splitting. **For SS sample,** the line width of radical E is large compared with other radical species and radicals A and B dominate together ESR spectrum. **For SMH samples**, three radical species were performed in the calculations, exhibiting isotropic (species A and H) and axially symmetric (species B) g tensors. It is seen that radical species A and B dominate the central part of the experimental spectrum; the radical H, with its small weight, gives rise to the appearance of the satellite lines of the very weak intensities. **For BHA samples,** for the simulation calculations two radical species named J and K were assumed and it is concluded that species J is produced more easily and therefore it dominates experimental spectrum. **For ALB samples,** simulation calculations were based on a model predicting the presence of two radical species where species M with its relatively high concentration and big linewidth dominates the ESR spectrum and species L has contributions to the peaks 1 and 2.

3.9. FT-IR studies

IR spectroscopy is also used as a complementary technique for ESR spectrocopy in the determination of the radical species induced upon irradiation for the investigated samples. For this purpose, FT-IR spectra of **SFZ**, **STZ**, and **SS** samples both for unirradiated and gamma-irradiated cases were recorded at room temperature. However, no significant differences between the unirradiated and irradiated IR spectra for the radical species created by gamma radiation were observed. Different spectra were also constructed using IR spectra of unirradiated and irradiated samples with using the same masses of the samples but still no meaningful results were obtained. Thus, it was concluded that the amounts of the radiation-induced intermediates were very small where they cannot create any significant detectable changes in the IR bands of the samples. This result is in agreement with that of relatively small G value (approximately, 0.1-0.5) calculated for the investigated samples by using ESR technique.

4. Conclusion

Experimental results derived for studied drugs/drug raw materials showed that they were not sensitive (small G value) to high energy radiations. Therefore, they could be sterilized by gamma radiation up to a radiation dose of 50 kGy without causing very much molecular damages upon irradiation. Also, they do not present the features of a good dosimetric material. That is, they cannot be used as an effective dosimetric material in the drug sterilization radiation dose limits. Nevertheless, the detection and discrimination of an unirradiated sample from irradiated samples turned out to be possible even at low radiation doses by ESR spectroscopy. Radical species created upon irradiation were found to decay much faster at stability conditions (40°C and 75% humidity) than at normal conditions as in the case of the samples in liquid forms. This point was considered presenting the possibility of diminishing even getting rid of radiolytical intermediates produced in irradiated samples. Therefore, it was concluded that gamma radiation produces relatively low amounts of radiolytic intermediates in the studies drugs/drug raw materials and that ESR spectroscopy could be used as a potential technique in monitoring the radiosterilization of drugs, drug raw materials, and drug delivery systems containing present samples as active ingredients.

Acknowledgements

I am grateful to **Prof. Dr. Mustafa Korkmaz** from Hacettepe University, Department of Physics Engineering, for sharing his excellent experience, for very valuable information and for his encouragement.

http://dx.doi.org/10.5772/61052

Author details

Şeyda Çolak*

Address all correspondence to: seyda@hacettepe.edu.tr

Hacettepe University, Physics Engineering Department, Ankara, Turkey

References

[1] Silva Aquino K. A. Sterilization by Gamma Irradiation, Gamma Radiation. In: Adrovic F. (ed.), Gamma Radiation. Rijeka: InTech; 2012. P171-206. Available from http://www.intechopen.com/books/gammaradiation/sterilization-by-gamma-irradiation in-chickpea (accessed 21 March 2012).

[2] Jacobs, G.P. A Review of the Effects of Gamma Radiation on Pharmaceutical Materials. J Biomater Applic 1995; 10 59-96.

[3] Reid, B. D. Gamma Processing Technology: An Alternative Technology for Terminal Sterilization of Parenterals. J Pharmaceut Sci Technol 1995; 49 (2) 83-89.

[4] Barbarin, N., Rollmann B. and Tilquin B. Role of Residual Solvents in the Formation of Volatile Compounds after Radiosterilization of Cefotaxime. Int J Pharmaceut 1999; 178 203-212.

[5] Boess, C. and Bögl K. W. Influence of Radiation Treatment on Pharmaceuticals - A Review: Alkaloids, Morphine Derivatives and Antibiotics. Drug Dev Indus Pharm 1996; 22 (6) 495-529.

[6] Maghraby A. M. Ionizing Radiation Induced Radicals. In: Nenoi M. (ed.) Current Topics in Ionizing Radiation Research. Rijeka: InTech; 2012. P649-682. Available from http://www.intechopen.com/books/current-topics-in-ionizing-radiation-research/ ionizing-radiation-inducedradicals- in-chickpea (accessed 12 February 2012).

[7] Pourahmad, R. and Pakravan, R. Radiosterilization of Disposable Medical Devices. Rad Phys Chem 1997; 49 285-286.

[8] Jacobs, G. Radiation in the Sterilization of Pharmaceuticals, Sterile Pharmaceutical Manufacturing. Buffalo Groze: Interpharm. Press; 1991.

[9] Duroux, J. L., Basly J. P., Penicaut, B. and Bernard M. ESR Spectroscopy Applied to the Study of Drugs Radiosterilization: Case of Three Nitroimidazoles. Appl Rad Isotopes 1996; 47 (11/12) 1565-1568.

[10] Bhalla H. L., Menon M. R. and Gopal N. G. S. Radiation Sterilization of Polyethylene Glycols. Int J Pharmaceut 1983; 17 351-355.

[11] Wogl, W. Radiation Sterilization of Pharmaceuticals, Chemical Changes and Consequences. Rad Phys Chem 1985; 25 425-435.

[12] Jacobs, G. P., Wills, P. A. Recent Developments in the Radiation Sterilization of Pharmaceuticals. Rad Phys Chem 1988; 31 685-691.

[13] Phillips, G. O. Radiation Technology in Surgery and Pharmaceutical Industry: An Overview of Applications. IAEA Bull 1994; 1 175-185.

[14] Varshney, L. and Patel K. M. Effects of Ionizing Radiations on a Pharmaceutical Compound Chloramphenicol. Rad Phys Chem 1994; 43 (5) 471-480.

[15] Safrany, A. Radiation Processing: Synthesis and Modification of Biomaterials for Medical Use. Nucl Instru Meth Phys Res B 1997; 131 376-381.

[16] Çolak Ş. and Korkmaz M. Investigation of Radiosterilization and Dosimetric Features of Sulfacetamide Sodium. J Pharmaceut Biomed Anal 2004; 36 791-798.

[17] Maksimenko, O., Pavlov, E., Toushov, E., Molin, A., Stukalov, Y., Prudskova, T., Feldman, V., Kreuter, J., Gelperina, S. Radiation Sterilization of Doxorubicin Bound to Poly(butyl cyanoacrylate) Nanoparticles. Int J Pharmaceut 2008; 356 325-332.

[18] Trends in Radiation Sterilization of Health Care Products, International Atomic Energy Agency, Vienna, 2008.

[19] EN 552, Sterilization of Medical Devices: Validation and Routine Control of Sterilization Irradiation, CEN, European Committee for Standardization, Brussels, Belgium; 1994.

[20] ISO 11137, Sterilization of Health Care Products: Requirements for Validation and Routine Control. Radiation Sterilization; International Organization for Standardization, Geneva, Switzerland; 1995.

[21] Gopal, N. G. S., Patel, K. M., Sharma, G., Bhalla, H.L., Wills, P. A., Hilmy, N. Guide for Radiation Sterilization of Pharmaceuticals and Decomposition of Raw Materials. Rad Phys Chem 1988; 32 619-622.

[22] Gibella, M., Crucq, A. S., Tilquin, B., Stocker, P., Lesgards, G. and Raffi, J. ESR Studies of Some Irradiated Pharmaceuticals. Rad Phys Chem 2000; 58 69-76.

[23] Schuler R. H. Three Decades of Spectroscopic Studies of Radiation Produced Intermediates. Rad Phys Chem 1994; 43 417-423.

[24] Miyazaki, T., Arai, J., Kaneko, K., Yamamoto, K., Gibella, M., Tilquin, B. Estimation of Irradiation Dose of Radiosterilized Antibiotics by ESR: Ampicillin. J Pharmaceut Sci 1994; 83 1643-1644.

[25] Bögl K. W. Identification of Irradiated Foods - Methods, Development and Concepts. Appl Rad Isotopes 1989; 40 1203-1210.

[26] Delincėe H. Analytical Methods for Irradiated Foods. A Review of Current Literature. IAEA-TECDOC-587, International Atomic Agency, Vienna; 1991.

[27] Desrosiers, M. F., Wilson, G. L., Hunter, C. R., Hutton, D. R. Estimation of the Absorbed Dose in Radiation-Processed Food. Part 1. Test of the EPR Response Function by a Linear Regression Analysis. Appl Rad Isotopes 1991; 42 613-616.

[28] Raffi, J. Delincėe, H., Marchioni E., Hasselmann C., Sjöberg A.M., Leonardi M., Kent M., Bögl K.W., Schreiber G., Stevenson H. and Meier W. Final Report on New Methods for the Detection of Irradiated Food, BCR, CEC, Luxembourg, EUR 15 261 EN; 1994.

[29] Ciranni Signoretti, E., Valvo L., Fattibene P., Onori S. and Pantoloni M. Gamma Radiation Induced Effects on Cefuroxime and Cefotaxime, Investigation on Degradation and Syn-Anti Isomerization. Drug Dev Indus Pharmacy 1994; 20 (16) 2493-2508.

[30] Onori S., Pantoloni M., Fattibene P., Ciranni Signoretti E., Valvo L. and Santucci M. ESR Identification of Irradiated Antibiotics: Cephalosporins. Appl Rad Isotopes 1996; 47 (11/12) 1569-1572.

[31] Çolak Ş., Maquille A., Tilquin B. Radiation Sterilization of Ketoprofen: ESR, HPLC, LC-MS, GC-MS Studies. Rad Effects Defects Solids 2006; 161 (1) 75-82.

[32] Hawkins, C. L., Davies, M. J. Detection and Characterisation of Radicals in Biological Materials using EPR Methodology. Biochim Biophys Acta 2014; 1840 708-721.

[33] Olguner Mercanoğlu G., Özer, A. Y., Çolak, Ş., Korkmaz, M., Barbarin, N., Tilquin, B., Özalp, M., Ekizoğlu, M. Radiosterilization of Sulfonamides I: Determination of the Effects of Gamma Irradiation on Solide Sulfonamides. Rad Phys Chem 2004; 69 511-520.

[34] Çolak Ş. and Korkmaz M. Investigation of Structural and Dynamic Features of the Radicals Produced in Gamma Irradiated Sulfanilamide: An ESR Study. Int J Pharmaceut 2003; 267 (1-2) 49-58.

[35] Çolak Ş. and Korkmaz M. Kinetics of the Radicals Induced in Gamma Irradiated Sulfafurazole: An EPR Study. Zeitschrift für Naturforschung 2004; 59a 481-487.

[36] Çolak Ş. and Korkmaz M. Spectroscopic Features of Radiolytical Intermediates Induced in Gamma Irradiated Sulfatiazole: An ESR Study. Int J Pharmaceut 2004; 285 1-11.

[37] Çolak Ş. and Korkmaz M. ESR Response of Gamma Irradiated Sulfamethazine. Rad Effects Defects Solids 2009; 164 (12) 788-799.

[38] Çolak Ş., Korkmaz M., Güneş Ç., Dölek, S. Investigation of Spectroscopic and Kinetic Features of the Radicals Produced in Gamma Irradiated Butylated Hydroxyanisole (BHA). Rad Effects Defects Solids 2009; 164 (2) 101-112.

[39] Çolak Ş. ESR Identification of Gamma Irradiated Albendazole. Rad Effects Defects Solids 2010; 165 (1) 72-82.

[40] Philips, G. O., Power, D. M. and Sewart, M. C. G. Effect of Gama Irradiation on Sodium Sulphacetamide. Rad Res 1971; 46 236-250.

[41] Philips, G. O.; Power, D. M. and Sewart, M. C. G. Effect of γ-Irradiation on Sulphonamides. Rad Res 1973; 53 204-215.

[42] Osol, A. Remington's Pharmaceutical Sciences. Easton: Mack Publishing; 1980.

[43] Tilquin, B. Composante Radicalaire des Transformations Radio-Initiées dans les Alcanes à 77 K. Thése d'agrégation. UCL, Ciaco-la-Neuve, Belgique;1985.

[44] Huzimura, R. ESR Studies of Radical Ion Centers in Irradiated $CaSO_4$. Jap J Appl Phys 1979; 18 2031-2032.

[45] Bershov, L. V., Martırsyan, V. O., Marfunin, A. S. and Speranskii, A. V. EPR and Structure Models for Radical Ions in Anhydrite Crystals. Fortschrıtte Der Mıneralogie 1975; 52 591-604.

[46] Samoilovich, M. I. and Tsinober, L. I. Characteristics of Radiation Color Centers and Microisomorphism in Crystals. Soviet Phys Crystallography 1970; 14 656-666.